

Stability and electronic properties of the LaNiO₂/SrTiO₃ interface

F. Bernardini¹ and A. Cano²

¹*Dipartimento di Fisica, Università di Cagliari, IT-09042 Monserrato, Italy*

²*Institut Néel, CNRS & UGA, 38042 Grenoble, France*

(Dated: July 3, 2022)

Infinite-layer nickelate thin films materialize an intriguing new platform for high-temperature unconventional superconductivity, with LaNiO₂/SrTiO₃ as reference setup. We discuss the relative stability of the elementary interfaces of this system and determine the corresponding electronic band structure. We find substantial changes compared to the bulk, in particular in relation to the 5*d* orbital contributions to the low-energy physics which can be totally replaced by purely Ni-3*d* flat bands. The *d*⁹ configuration characteristic of cuprates can thus be supplemented by an extra interfacial ingredient destabilizing the normal non-superconducting state in these heterostructures.

Infinite-layer nickelates have long been proposed as intriguing analogues to high-*T_c* superconducting cuprates, thus sustaining a rather fundamental research on these systems over the years [1–6]. As a result of such a “niche” background activity, superconductivity has recently been reported in Sr-doped NdNiO₂/SrTiO₃ thin films [7]. This finding represents an important breakthrough that, however, seems to be remarkably difficult to reproduce. In fact, the reported *T_c*’s vary quite substantially from sample to sample, even if they are nominally equivalent, and no definitive result is given for the LaNiO₂/SrTiO₃ case [7]. Beyond that, no superconductivity has been found in epitaxial thin films directly grown on SrTiO₃ and alternative substrates and, very importantly, in bulk samples so far [8, 9]. This state of affairs calls for the investigation of the corresponding interface itself since it can play a non-trivial role in the reported superconductivity.

Here, we investigate theoretically the fundamental properties of the reference LaNiO₂/SrTiO₃ interface by means of density functional theory (DFT) calculations. This system is expected to be representative for the infinite-layer nickelate series without requiring any ambiguous treatment of 4*f* electrons [2, 3, 10–12]. We model the interface by a symmetric supercell with two identical interfacial layers among the four elementary possibilities illustrated in Fig. 1. Our model is also fully relevant for the ultrathin limit of these systems, as one full LaNiO₂ layer is always sandwiched between the interfaces. Thus, we determine the most stable interfacial configuration according to the corresponding thermodynamics. As we show below, the fragile stability of the infinite-layer bulk nickelates manifests also through the marked differences in the relative energetics of the heterostructure. Thus, the growth process can be expected to have a non-negligible impact on the eventual atomic configuration that is realized experimentally. In addition, we study the specific features that emerge in the local band structure as a function of such an atomic configuration. We find drastic changes compared to the bulk. In particular, while the Ni-3*d*_{*x*²-*y*²} low-energy features are robust against interfacial effects, the metallic character provided by the La-5*d* states in the bulk can be replaced either by Ti-3*d* contributions or directly by Ni-3*d*_{*z*²} flat

bands in the ultrathin limit. This modifies qualitatively the initial picture for the development of strong correlations and the eventual Cooper pairing, which then might display a distinct interfacial nature in infinite-layer nickelates of this class.

I. COMPUTATIONAL METHODS

We performed density functional theory (DFT) calculations to investigate the LaNiO₂/SrTiO₃ heterostructure. We considered a tetragonal supercell with 3 Ni and 3 Ti atoms and two identical boundary layers, simulating the epitaxial LaNiO₂ by imposing the calculated latticed parameters of bulk SrTiO₃ ($a = b = 3.94 \text{ \AA}$). The *c* lattice parameter, in its turn, was optimized using a constrained variable-cell dynamics. We used the VASP code [13] for these calculations with the PBE [14] exchange-correlation functional and PAW pseudo-potentials [15]. We employed a plane-wave cutoff of 540 eV and a Monkhorst-Pack $6 \times 6 \times 2$ *k*-mesh with a 0.2 eV Gaussian smearing, and treated the Sr-4*s*4*p*, Ti-3*s*3*p* and Ni-3*p* electrons as valence electrons. The convergence criteria were 1 meV on the total energy, 0.001 Å on the *c* parameter, 0.01 eV/Å on the residual forces. The structural parameters of the supercells are summarized in Table I. The corresponding chemical potentials are determined below from analogous total energy calculations of equilibrium bulk structures using the same plane-wave cutoff and smearing, and a *k*-mesh equivalent to a cubic $6 \times 6 \times 6$ one whenever possible. The results are summarized in Table II.

The electronic band structure was further computed using the full-potential linear augmented plane-wave (FLAPW) method as implemented in the WIEN2K package [16], with the LDA exchange-correlation functional [17]. We performed spinless calculations with muffin-tin radii of 2.5 a.u., 2.1 a.u., 2.0 a.u. and 1.5 a.u. for the La (Sr), Ni, Ti and O atoms respectively and a plane-wave cutoff $R_{\text{MT}}K_{\text{max}} = 7.0$. The integration over the Brillouin zone was performed using a $13 \times 13 \times 2$ *k*-mesh for the self-consistent calculations, while a denser $36 \times 36 \times 6$ *k*-mesh was used for the Fermi surface.

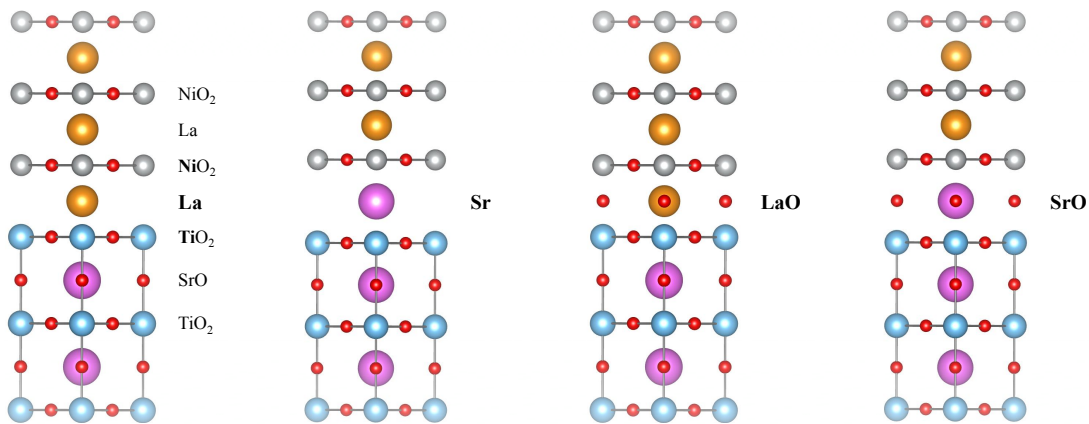


FIG. 1. Ball-and-stick model of the elementary LaNiO₂/SrTiO₃ interfaces. The boundary layer can be made of either La, Sr, LaO, or SrO planes as indicated in the figure. The interfacial atoms indicated with bold symbols are denoted by the i subscript in the main text.

	La	Sr	LaO	SrO
c (Å)	21.82	21.89	22.5	22.70
Ni _{i} -O (Å)	3.745	3.723	3.736	3.768
O _{i} -Ni _{i} (Å)	-	-	4.151	3.716
\angle O _{i} -Ni _{i} -O (°)	-	-	85.07	98.95
E_{tot} (eV)	-201.07	-192.92	-218.69	-209.13

TABLE I. Structural parameters and total energy of the supercells used to study the four elementary LaNiO₂/SrTiO₃ interfaces sketched in Fig. 1. Ni _{i} denotes the first nickel next to the interfacial layer and O _{i} the interfacial oxygen (bold symbols in Fig. 1). The reported values correspond to the overall c parameter, O _{i} -Ni _{i} distance, Ni _{i} -O distance, and O _{i} -Ni _{i} -O bond angle.

	ΔH_f (eV)	E_{tot} (eV)	a (Å)	c (Å)	Space group
LaNiO ₃	-12.27	-35.90	3.829	3.829	$P4/mmm$
LaNiO ₂	-9.77	-28.96	3.936	3.393	$P4/mmm$
LaNiO	-5.42	-20.18	3.584	3.842	$P4/mmm$
La ₂ O ₃	-18.78	-41.84	3.937	6.181	$P6_3/mmc$
NiO	-1.48	-11.36	4.151	4.151	$Fm\bar{3}m$
La	-	-4.88	3.767	12.129	$P6_3/mmc$
Ni	-	-5.44	3.499	3.499	$Fm\bar{3}m$
SrTiO ₃	-17.35	-40.11	3.940	3.940	$Pm\bar{3}m$
SrO	-5.99	-12.06	5.203	5.203	$Fm\bar{3}m$
TiO ₂	-9.17	-25.87	4.160	8.579	$I4_1/amd$
Sr	-	-1.64	6.038	6.038	$Fm\bar{3}m$
Ti	-	-7.84	2.939	4.640	$P6_3/mmc$

TABLE II. Formation enthalpy and structural parameters of the different compounds used to determine the chemical potentials that define the interface energy according to Eq. (1). The formation enthalpy of LaNiO₂, for example, is defined as $\Delta H_f^{\text{LaNiO}_2} = E_{\text{tot}}^{\text{LaNiO}_2} - E_{\text{tot}}^{\text{La}} - E_{\text{tot}}^{\text{Ni}} - E_{\text{tot}}^{\text{O}_2}$, and a similar definition applies for the rest of compounds.

II. STRUCTURE OF THE INTERFACE

We first address the question of the actual structure of the LaNiO₂/SrTiO₃ interface. We assume the ideal case in which the interface is not modified by e.g. oxygen vacancies or topotactic hydrogens [18], and such that no interface reconstruction takes place. In fact, in (001) oriented SrTiO₃ substrates, ideal SrO and TiO₂ terminated surfaces are the most stable configurations according to first-principles calculations [19] and they regularly are realized experimentally [20]. In addition, the closely related LaAlO₃/SrTiO₃ system for example displays a well defined LaO flat interface (see e.g. [21, 22]).

In order to determine the relative formation energy of the four LaNiO₂/SrTiO₃ elementary interfaces (see Fig. 1) we follow the thermodynamic approach described in [23–25]. Thus we define the interface energy as

$$E_{\text{interface}} = \frac{1}{2} \left(E_{\text{tot}} - \sum_{X=\text{La, Ni, O, Sr, Ti}} \mu_X N_X \right), \quad (1)$$

where E_{tot} is the total energy of the corresponding supercell, μ_X is the chemical potential of the X element, and N_X is the number of X atoms in the supercell.

Consider first the La and LaO interfaces. Their energy difference can be written as

$$\begin{aligned} \Delta E_{\text{interface}}^{\text{La-LaO}} &= \frac{1}{2} (E_{\text{tot}}^{(\text{La})} - E_{\text{tot}}^{(\text{LaO})}) + \mu_{\text{O}} \\ &= \frac{1}{2} (E_{\text{tot}}^{(\text{La})} - E_{\text{tot}}^{(\text{LaO})} + E_{\text{tot}}^{\text{O}_2}) + \Delta\mu_{\text{O}}. \end{aligned} \quad (2)$$

Here and hereafter $\Delta\mu_X \leq 0$ denotes the chemical potential of X relative to its value in the most stable elementary phase of X (that is, $2\Delta\mu_{\text{O}} = 2\mu_{\text{O}} - E_{\text{tot}}^{\text{O}_2}$ in the case of X = O). As we see, the relative stability of these two interfaces can be defined in terms of the oxygen chemical potential $\Delta\mu_{\text{O}}$. We find that the LaO interface will be favored over the La one if $\Delta\mu_{\text{O}} > -4.38$ eV (and vice

versa). Similarly, we find that the SrO interface will be favored over the Sr one if $\Delta\mu_{\text{O}} > -3.67$ eV.

The actual value of $\Delta\mu_{\text{O}}$ can be narrowed down from the following considerations. On one hand, the overall thermodynamics has to be such that LaNiO_2 is more stable than LaNiO_3 in the conditions under consideration. That is, $\Delta H_f^{\text{LaNiO}_2} < \Delta H_f^{\text{LaNiO}_3} - \Delta\mu_{\text{O}}$. At the same time, LaNiO_2 must be more stable than $\text{LaNiO} + \text{O}$. That is, $\Delta H_f^{\text{LaNiO}_2} < H_f^{\text{LaNiO}} + \Delta\mu_{\text{O}}$. Taken together, these two conditions tell us that

$$\underbrace{-4.35 \text{ eV}}_{\Delta H_f^{\text{LaNiO}_2} - \Delta H_f^{\text{LaNiO}}} < \Delta\mu_{\text{O}} < \underbrace{-2.50 \text{ eV}}_{\Delta H_f^{\text{LaNiO}_3} - \Delta H_f^{\text{LaNiO}_2}} \quad (3)$$

according to the enthalpies listed in Table II. These limits can be understood as associated to oxygen-poor and oxygen-rich conditions respectively. We note that NiO is never stable within such a $\Delta\mu_{\text{O}}$ interval, so that we can assume $\Delta\mu_{\text{Ni}} < 0$ in the following. Beyond that, we can already conclude that the LaO interface is always energetically favorable compared to the La one (even if they become essentially degenerate in the extreme oxygen-poor limit).

Consider now the LaO and SrO interfaces:

$$\Delta E_{\text{interface}}^{\text{SrO-LaO}} = \frac{1}{2} \left(E_{\text{tot}}^{(\text{SrO})} - E_{\text{tot}}^{(\text{LaO})} \right) + E_{\text{tot}}^{\text{La}} - E_{\text{tot}}^{\text{Sr}} + \Delta\mu_{\text{La}} - \Delta\mu_{\text{Sr}}, \quad (4)$$

and the LaO and Sr ones:

$$\Delta E_{\text{interface}}^{\text{Sr-LaO}} = \frac{1}{2} \left(E_{\text{tot}}^{(\text{Sr})} - E_{\text{tot}}^{(\text{LaO})} + E_{\text{tot}}^{\text{O}_2} \right) + E_{\text{tot}}^{\text{La}} - E_{\text{tot}}^{\text{Sr}} + \Delta\mu_{\text{La}} - \Delta\mu_{\text{Sr}} + \Delta\mu_{\text{O}}. \quad (5)$$

According to the computed values of the total energies we find that the LaO interface is energetically favored with respect to the SrO one if $\Delta\mu_{\text{La}} - \Delta\mu_{\text{Sr}} > -1.54$ eV, and this is also the case with respect to the Sr one if $\Delta\mu_{\text{La}} - \Delta\mu_{\text{Sr}} + \Delta\mu_{\text{O}} > -5.21$ eV. In fact, these potentials need to be such that

$$\min \Delta\mu_{\text{La}} = \Delta H_f^{\text{LaNiO}_2} - \max \Delta\mu_{\text{Ni}} - 2\Delta\mu_{\text{O}}, \quad (6)$$

$$\max \Delta\mu_{\text{Sr}} = \Delta H_f^{\text{SrO}} - \Delta\mu_{\text{O}}. \quad (7)$$

By subtracting these equations and using Table II we find that

$$\min[\Delta\mu_{\text{La}} - \Delta\mu_{\text{Sr}}] + \Delta\mu_{\text{O}} = \underbrace{-3.78 \text{ eV}}_{\Delta H_f^{\text{LaNiO}_2} - \Delta H_f^{\text{SrO}}}. \quad (8)$$

Taking into account (3), this further yields

$$-1.12 \text{ eV} < \min[\Delta\mu_{\text{La}} - \Delta\mu_{\text{Sr}}] < 0.57 \text{ eV}. \quad (9)$$

As we see, among the four possible configurations, the LaO layer always minimizes the interface energy since $\Delta\mu_{\text{La}} - \Delta\mu_{\text{Sr}}$ and $\Delta\mu_{\text{La}} - \Delta\mu_{\text{Sr}} + \Delta\mu_{\text{O}}$ are always too high to promote any of the other possibilities within the allowed range of $\Delta\mu_{\text{O}}$.

What we have discussed so far applies to the direct formation of the $\text{LaNiO}_2/\text{SrTiO}_3$ interface as obtained in [8] for example. However, such a heterostructure can also be obtained by means of the two-step process employed in [7]. That is, by first growing the LaNiO_3 perovskite on top of the SrTiO_3 substrate, and then applying a topotactic reduction process to obtain LaNiO_2 out of it. In this case, the only elemental boundaries between the two perovskites are either the LaO interface or the SrO one, and a slightly different rationale has to be applied to determine their relative stability as detailed in the Supporting Information. Thus, we find that the LaO interface will again be the most energetically favorable one under oxygen-poor conditions. However, in contrast to the direct process, there is now room for stabilizing the SrO one in the oxygen-rich case. If the SrO interface between the two perovskites is eventually realized, then the Sr one can also be obtained after the second step — *i.e.* via the subsequent reduction process — since it can be compatible with the final thermodynamics if the LaO interface is thus bypassed.

III. ELECTRONIC BAND STRUCTURE

Next, we discuss the electronic band structure of the $\text{LaNiO}_2/\text{SrTiO}_3$ heterostructure as a function of the morphology of the interface. Fig. 2 show the calculated dispersion across the two-dimensional Brillouin zone of the interface and perpendicular to it. We find important changes with respect to the bulk material near the Fermi level depending on the interfacial configuration. These changes can be better understood in relation to the local atomic structure of the interfacial layer. In our calculations, the interfaces are embedded in supercells containing 2 equivalent interfacial Ni_i atoms + 1 “bulk” Ni atoms (surrounded by 1 O_i + 4 O and 4 O atoms respectively, see Fig. 1).

It is instructive to start with the La and Sr interfaces, even if they are the most unlikely configurations according to the overall thermodynamics discussed in the previous section. In fact, the La case can be anticipated to be rather similar to the bulk since the local environment of the interfacial Ni_i is essentially the same. This is confirmed in Fig. 2 where, in addition to the Ni_i - $3d_{x^2-y^2}$ bands crossing the Fermi level, we also observe the self-doping effect due to the La_i - $5d_{z^2}$ ones. These are the main features of the bulk, which are thus preserved at the interface in such a La configuration. The main change is observed at the M point, where two additional bands can be seen near the Fermi level. Their Ni_i orbital character is $3d_{z^2}$ and $3d_{xz/yz}$ along the X - M - Γ line. These features result from the mixing with the La_i - $5d_{xy}$ bands, which now provide an important extra contribution to the La - $5d_{z^2}$ electron self-doping at this interface.

In the case of the Sr interface we observe essentially the same features. The main difference now is the slight

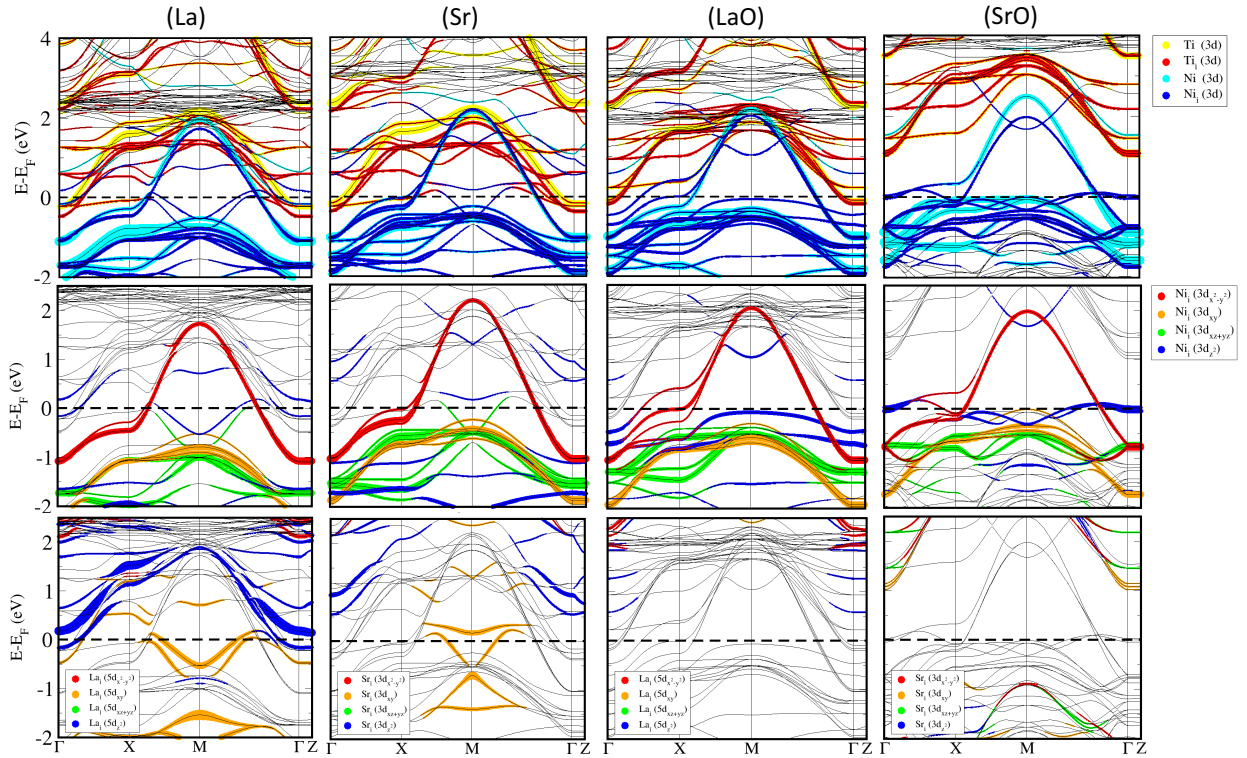


FIG. 2. Layer-projected (top) and orbital-resolved (middle and bottom) band structure of the $\text{LaNiO}_2/\text{SrTiO}_3$ symmetric supercells for different interfacial configurations.

overall shift upwards of the bands and, in particular, of their $\text{Ni-}3d_{z^2}$ character. This is totally in tune with the interfacial hole-doping that results from the $\text{La} \rightarrow \text{Sr}$ local substitution at the interface. This substitution, in addition, has a striking impact on the electron-self doping effect at the interface, which is now entirely provided by $\text{Ti}_i\text{-}3d$ states at Γ (rather than by $\text{Sr}_i\text{-}3d$ ones). Thus, the nature of the metallic character of the system is locally modified by the interfacial configuration.

In the LaO case, more substantial changes are also obtained in the Ni_i bands. First of all, the shift upwards of the originally $\text{Ni-}3d_{z^2}$ bands is more pronounced. The mixing with the $\text{Ni-}3d_{x^2-y^2}$ ones is thus enhanced and this is accompanied with an important splitting of the Ni and Ni_i bands along the $\Gamma\text{-X-M}$ path about the Fermi level. These features are in fact associated to avoided band crossings that are best exemplified in bulk fluoronickelates counterparts [26]. The crossing of these bands with the Fermi level is still dominated by the $\text{Ni}_i\text{-}3d_{x^2-y^2}$ orbitals, even if there is a rather flat $\text{Ni}_i\text{-}3d_{z^2}$ band right below E_F at the M point. Beyond that, the bands intersecting the Fermi level at Γ have a $\text{Ti}_i\text{-}3d$ character. Again this is in striking contrast to the bulk and can be associated to the interfacial LaO layer itself.

In the case of SrO, the shift upwards of the $\text{Ni}_i\text{-}3d_{z^2}$ bands is even more pronounced and the eventual situation is such that only the Ni bands intersect the Fermi level. They now have both $3d_{x^2-y^2}$ and $3d_{z^2}$ orbital contributions. The new bands intersecting the Fermi level

are remarkably flat, which is compatible with the formation of a genuine interfacial band localized at the SrO plane. Importantly, there is no electron self-doping effect due to neither $\text{Ti-}3d$ nor $\text{La-}5d$ contributions in this case. The absence of these contributions is an important qualitative difference compared to the previous configurations and the bulk.

In both LaO and SrO configurations the interfacial Ni_i is surrounded by an extra oxygen O_i compared to the bulk Ni. This oxygen will tend to take one electron from Ti_i and the other from Ni_i . Thus, the $\text{Ni}_i\text{-O}_i$ bond will have an important contribution from the $\text{Ni-}3d_{z^2}$ orbitals. Taking into account the rather asymmetric arrangement of the Ni_i environment, this can be expected to yield both bondings and backbondings. In fact, in both LaO and SrO configurations, the flat $\text{Ni}_i\text{-}3d_{z^2}$ band can be associated to such bondings while the empty parabolic band bent upwards with $\text{Ni}_i\text{-}3d_{z^2}$ character at M can be associated to the backbondings. The Ni_i will thus tend to feature a nominal Ni_i^{2+} oxidation state in the LaO case (where it is surrounded by 8 La) and $\text{Ni}_i^{2.5+}$ in SrO (where it has 4 La and 4 Sr nearby, the latter providing an extra 0.5 hole doping). The extra electrons given by the Ni_i will come from the $3d_{x^2-y^2}$ orbitals, as usual, and from the $3d_{z^2}$ ones via the interfacial oxygen O_i . This explains the shift upwards of the $\text{Ni}_i\text{-}3d_{z^2}$ bands up to the Fermi level. At the same time, this naturally yields a reduced splitting between $\text{Ni-}3d$ and $\text{O-}2p$ levels (i.e. charge-transfer energies) compared to the bulk. This re-

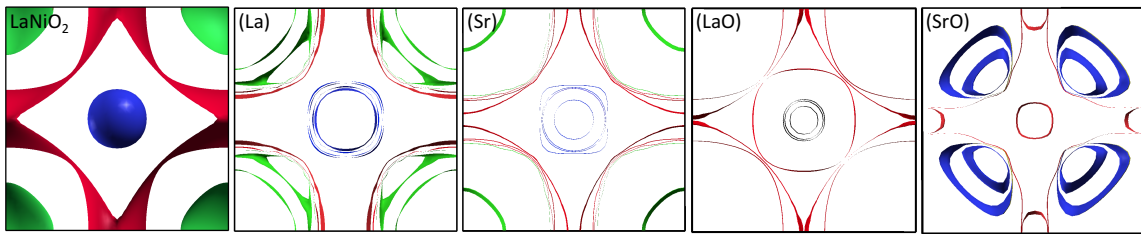


FIG. 3. Top view of the Fermi surface of bulk LaNiO_2 and of the $\text{LaNiO}_2/\text{SrTiO}_3$ heterostructure for the different elementary configurations of the interfacial layer.

duction is such that even a non-negligible $\text{O}_i\text{-}2p$ contribution to density of states eventually emerges at the Fermi energy in the SrO case. Thus, in some sense, these interfacial configurations locally bridge the ‘charge-transfer vs Mott insulator’ gap between bulk cuprates and nickelates [10, 27].

The corresponding Fermi surfaces are shown in Fig. 3. The La, Sr, and LaO configurations yield a sort of direct 2D version of LaNiO_2 Fermi surface. However, the initial electron pockets at Γ (La- $5d$ in the La case as in the bulk) are dominated by Ti- $3d$ orbitals in Sr and LaO, and disappear in SrO. The La and Sr interfaces produce additional pockets at M due to Ni- $3d$ contributions mixed with La- $5d$ and Sr- $3d$ respectively. Most importantly, in the SrO case the initial La- $5d$ pockets at Γ disappear and there appears a series of extra pockets along the Γ - M path. These new pockets are associated to a flat Ni- $3d_{z^2}$ band, which is the most distinct feature of the SrO interfacial configuration.

IV. CONCLUSIONS

Infinite-layer nickelate thin films offer an intriguing new platform for unconventional high-temperature superconductivity, with important analogies and differences with respect to the classic case of cuprates. Our work clarifies the specific fundamental features that emerge at the interface and in the ultrathin limit of these systems. To illustrate these features, we have performed a detailed analysis of the reference $\text{LaNiO}_2/\text{SrTiO}_3$ heterostructure. The fragile stability of the infinite-layer nickelates in the bulk is found to have a peculiar impact on the ener-

getics of the elementary interfaces. Thus, while the direct growth of epitaxial films is expected to yield LaO as the most stable interfacial configuration, their two-step synthesis via perovskite precursors is found to be compatible with both SrO and Sr interfacial layers too. This has important consequences for the overall electronic band structure that is eventually realized in these films. These can be linked to the local environment of the interfacial Ni atoms. The most ‘‘bulk-like’’ boundary layer corresponds to the La interfacial configuration, which in fact preserves the main band-structure features of the bulk. The interfacial La \rightarrow Sr replacement, however, produces a striking change in the nature of the metallic character of the system, as the extra La- $5d$ contribution becomes Ti- $3d$ at the interface. The LaO configuration, in addition, implies an enhanced mix of the Ni- $3d_{x^2-y^2}$ and Ni- $3d_{z^2}$ orbitals near the Fermi level. While this has been argued to be detrimental for superconductivity in cuprates [28], the interfacial Ni- $3d_{z^2}$ bands display a remarkable flattening that, by analogy to twisted bilayer graphene and graphite interfaces for example [29, 30], could result into an additional superconducting instability. The SrO interface gives rise to the most dramatic changes. In this case the low-energy physics in the ultrathin limit is in fact entirely determined by Ni- $3d$ electrons, with the original Ni- $3d_{x^2-y^2}$ features now supplemented by the interfacial Ni- $3d_{z^2}$ flat bands exclusively. This changes qualitatively the picture for the subsequent emergence of superconductivity, as the presence of these flat bands need to be fully considered. Thus, our findings are expected to motivate new perspectives for further theoretical and experimental work on infinite-layer nickelates.

Acknowledgments. The authors are grateful to V. Olevano and X. Blase for insightful discussions.

-
- [1] M. A. Hayward, M. A. Green, M. J. Rosseinsky, and J. Sloan, *Journal of the American Chemical Society* **121**, 8843 (1999), <https://doi.org/10.1021/ja991573i>.
 [2] V. I. Anisimov, D. Bukhvalov, and T. M. Rice, *Phys. Rev. B* **59**, 7901 (1999).
 [3] K.-W. Lee and W. E. Pickett, *Phys. Rev. B* **70**, 165109 (2004).
 [4] M. Crespin, O. Isnard, F. Dubois, J. Choisnet, and

- P. Odier, *Journal of Solid State Chemistry* **178**, 1326 (2005).
 [5] J. Zhang, A. S. Botana, J. W. Freeland, D. Phelan, H. Zheng, V. Pardo, M. R. Norman, and J. F. Mitchell, *Nature Phys.* **13**, 864 (2017).
 [6] A. S. Botana, V. Pardo, and M. R. Norman, *Phys. Rev. Materials* **1**, 021801 (2017).
 [7] D. Li, K. Lee, B. Y. Wang, M. Osada, S. Crossley, H. R.

- Lee, Y. Cui, Y. Hikita, and H. Y. Hwang, *Nature* **572**, 624 (2019).
- [8] X. Zhou, Z. Feng, P. Qin, H. Yan, S. Hu, H. Guo, X. Wang, H. Wu, X. Zhang, H. Chen, X. Qiu, and Z. Liu, [arXiv:1911.04662](#).
- [9] Q. Li, C. He, J. Si, X. Zhu, Y. Zhang, and H.-H. Wen, [arXiv:1911.02420](#).
- [10] A. S. Botana and M. R. Norman, [arXiv:1908.10946](#).
- [11] H. Sakakibara, H. Usui, K. Suzuki, T. Kotani, H. Aoki, and K. Kuroki, [arXiv:1909.00060](#).
- [12] F. Bernardini, V. Olevano, and A. Cano, [arXiv:1910.13269](#).
- [13] G. Kresse and J. Furthmuller, *Computational Materials Science* **6**, 15 (1996).
- [14] J. P. Perdew, K. Burke, and M. Ernzerhof, *Phys. Rev. Lett.* **77**, 3865 (1996).
- [15] G. Kresse and D. Joubert, *Phys. Rev. B* **59**, 1758 (1999).
- [16] P. Blaha, K. Schwarz, G. Madsen, D. Kvasnicka, J. Luitz, R. Laskowski, F. Tran, and L. D. Marks, WIEN2k, An Augmented Plane Wave + Local Orbitals Program for Calculating Crystal Properties (Karlheinz Schwarz, Techn. Universitt Wien, Austria), 2018. ISBN 3-9501031-1-2.
- [17] J. P. Perdew and A. Zunger, *Phys. Rev. B* **23**, 5048 (1981).
- [18] L. Si, W. Xiao, J. Kaufmann, J. M. Tomczak, Y. Lu, Z. Zhong, and K. Held, [arXiv:1911.06917](#).
- [19] E. Heifets, S. Piskunov, E. A. Kotomin, Y. F. Zhukovskii, and D. E. Ellis, *Phys. Rev. B* **75**, 115417 (2007).
- [20] K. Szot and W. Speier, *Phys. Rev. B* **60**, 5909 (1999).
- [21] V. Vonk, M. Huijben, K. J. I. Driessen, P. Tinnemans, A. Brinkman, S. Harkema, and H. Graafsma, *Phys. Rev. B* **75**, 235417 (2007).
- [22] R. Pentcheva and W. E. Pickett, *Phys. Rev. B* **78**, 205106 (2008).
- [23] G.-X. Qian, R. M. Martin, and D. J. Chadi, *Phys. Rev. B* **38**, 7649 (1988).
- [24] N. Chetty and R. M. Martin, *Phys. Rev. B* **45**, 6089 (1992).
- [25] C. G. Van de Walle, D. B. Laks, G. F. Neumark, and S. T. Pantelides, *Phys. Rev. B* **47**, 9425 (1993).
- [26] F. Bernardini, V. Olevano, X. Blase, and A. Cano, [arXiv:1911.11788](#).
- [27] M. Jiang, M. Berciu, and G. A. Sawatzky, [arXiv:1909.02557](#).
- [28] H. Sakakibara, H. Usui, K. Kuroki, R. Arita, and H. Aoki, *Phys. Rev. B* **85**, 064501 (2012).
- [29] N. B. Kopnin, T. T. Heikkilä, and G. E. Volovik, *Phys. Rev. B* **83**, 220503 (2011).
- [30] See e.g. G. E. Volovik, and the references therein., [arXiv:1803.08799](#).

SUPPORTING INFORMATION

Relative stability of the LaNiO₃/SrTiO₃ interfaces

The elementary LaNiO₃/SrTiO₃ interface between the two perovskites can only be in either LaO or SrO configurations in the absence of surface reconstruction. Their energy difference can be written as (4), where the total energies are now associated to the corresponding perovskite supercells. Accordingly, we find that the LaO interface will be energetically favored over the SrO one if $\Delta\mu_{\text{La}} - \Delta\mu_{\text{Sr}} > -2.35$ eV and *vice versa*.

The interval of thermodynamically allowed values for such a difference of chemical potentials further depends on $\Delta\mu_{\text{O}}$ and $\Delta\mu_{\text{Ni}}$, and can be determined as follows. First of all, note that $\Delta\mu_{\text{O}}$ should be high enough so that LaNiO₃ does not decompose into LaNiO₂. That is

$$\Delta H_f^{\text{LaNiO}_3} < \Delta H_f^{\text{LaNiO}_2} + \Delta\mu_{\text{O}}. \quad (10)$$

According to the enthalpies listed in Table II that means -2.50 eV $< \Delta\mu_{\text{O}}$. In addition, LaNiO₃ should also be stable with respect its decomposition into La₂O₃ and NiO. In fact, if -2.50 eV $< \Delta\mu_{\text{O}}$, then the inequality $H_f^{\text{LaNiO}_3} < \frac{1}{2}\Delta H_f^{\text{La}_2\text{O}_3} + \Delta H_f^{\text{NiO}} + \frac{1}{2}\Delta\mu_{\text{O}}$ is always satisfied. Regarding $\Delta\mu_{\text{Ni}} \leq 0$, its lower bound given by the condition that LaNiO₃ should not decompose into La₂O₃, free O and metallic Ni:

$$H_f^{\text{LaNiO}_3} < \frac{1}{2}\Delta H_f^{\text{La}_2\text{O}_3} + \frac{3}{2}\Delta\mu_{\text{O}} + \Delta\mu_{\text{Ni}} \quad (11)$$

Thus, the minimum value for $\Delta\mu_{\text{Ni}}$ will be:

$$\Delta\mu_{\text{Ni}}^{\min} = H_f^{\text{LaNiO}_3} - \frac{1}{2}\Delta H_f^{\text{La}_2\text{O}_3} - \frac{3}{2}\Delta\mu_{\text{O}}. \quad (12)$$

The lowest and highest values for $\Delta\mu_{\text{La}}$ are then obtained by the equilibrium condition for the existence of the LaNiO₃ bulk:

$$\Delta\mu_{\text{La}}^{\min} = \Delta H_f^{\text{LaNiO}_3} - \Delta\mu_{\text{Ni}}^{\max} - 3\Delta\mu_{\text{O}}, \quad (13)$$

$$\Delta\mu_{\text{La}}^{\max} = \Delta H_f^{\text{LaNiO}_3} - \Delta\mu_{\text{Ni}}^{\min} - 3\Delta\mu_{\text{O}}. \quad (14)$$

Eq. 14 must be used with caution. Indeed using the values given in Table II we obtain a positive value of $\Delta\mu_{\text{La}}^{\text{max}}$ for $\Delta\mu_{\text{O}} > -1.92$ eV. This is incompatible with the fact that the chemical potentials are such that $\Delta\mu_{\text{X}} < 0$. Consequently, for O-rich values $\Delta\mu_{\text{O}} > -1.92$ eV we can safely put $\Delta\mu_{\text{La}}^{\text{max}} = 0$.

As for the SrTiO₃ crystal we find it stable for values of $\Delta\mu_{\text{O}}$ well below -2.5 eV [19]. No concern exists about the possible decomposition of SrTiO₃ into SrTiO₂. The upper values of the chemical potentials of Sr and Ti are limited by the condition of unfavourable formation of SrO and TiO₂:

$$\Delta\mu_{\text{Sr}} < \Delta H_f^{\text{SrO}} - \Delta\mu_{\text{O}} = \Delta\mu_{\text{Sr}}^{\text{max}}, \quad (15)$$

$$\Delta\mu_{\text{Ti}} < \Delta H_f^{\text{TiO}_2} - 2\Delta\mu_{\text{O}} = \Delta\mu_{\text{Ti}}^{\text{max}}. \quad (16)$$

Inserting $\Delta\mu_{\text{Ti}}^{\text{max}}$ in the equilibrium condition for SrTiO₃ we obtain the lowest value for $\Delta\mu_{\text{Sr}}$ as

$$\Delta\mu_{\text{Sr}}^{\text{min}} = H_f^{\text{SrTiO}_3} - \Delta\mu_{\text{Ti}}^{\text{max}} - 3\Delta\mu_{\text{O}}. \quad (17)$$

The allowed range of $\Delta\mu_{\text{La}} - \Delta\mu_{\text{Sr}}$ are determined by the lowest and highest values of the chemical potentials $\Delta\mu_{\text{La}}$ and $\Delta\mu_{\text{Sr}}$. Subtracting Eq. 15 from Eq. 13 we obtain the lowest value for $\Delta\mu_{\text{La}} - \Delta\mu_{\text{Sr}}$ as

$$\Delta\mu_{\text{La}}^{\text{min}} - \Delta\mu_{\text{Sr}}^{\text{max}} = \Delta H_f^{\text{LaNiO}_3} - \Delta H_f^{\text{SrO}} - 2\Delta\mu_{\text{O}}. \quad (18)$$

while subtracting Eq. 17 from Eq. 14 we obtain its highest value. The latter is

$$\Delta\mu_{\text{La}}^{\text{max}} - \Delta\mu_{\text{Sr}}^{\text{min}} = \Delta H_f^{\text{LaNiO}_3} - \Delta H_f^{\text{SrTiO}_3} + \Delta H_f^{\text{TiO}_2} - 2\Delta\mu_{\text{O}}. \quad (19)$$

in O-poor conditions ($\Delta\mu_{\text{O}} = -2.50$ eV) and

$$\Delta\mu_{\text{La}}^{\text{max}} - \Delta\mu_{\text{Sr}}^{\text{min}} = \frac{1}{2}\Delta H_f^{\text{La}_2\text{O}_3} - \Delta H_f^{\text{SrTiO}_3} + \Delta H_f^{\text{TiO}_2} - \frac{1}{2}\Delta\mu_{\text{O}}. \quad (20)$$

in O-rich conditions ($\Delta\mu_{\text{O}} = 0$). Using the values listed in Table II we find that in O-poor conditions

$$-1.28 \text{ eV} < \Delta\mu_{\text{La}} - \Delta\mu_{\text{Sr}} < +0.91 \text{ eV}, \quad (21)$$

while in O-rich conditions we have

$$-6.28 \text{ eV} < \Delta\mu_{\text{La}} - \Delta\mu_{\text{Sr}} < -1.21 \text{ eV}. \quad (22)$$

Thus we conclude that, while the most energetically favorable interface is always the LaO one in O-poor conditions, both LaO and SrO interfaces can be formed in the O-rich case.